

Antenna Selection in MIMO Non-Orthogonal Multiple Access Systems

Yuehua Yu, He Chen, Yonghui Li, Zhiguo Ding, Lingyang Song, and Branka Vucetic

Abstract—This paper considers the antenna selection (AS) problem for a MIMO non-orthogonal multiple access (NOMA) system. In particular, we develop new computationally-efficient AS algorithms for two commonly-used scenarios: NOMA with fixed power allocation (F-NOMA) and NOMA with cognitive radio-inspired power allocation (CR-NOMA), respectively. For the F-NOMA scenario, a new max-max-max antenna selection (A^3 -AS) scheme is firstly proposed to maximize the system sum-rate. This is achieved by selecting one antenna at the base station (BS) and corresponding best receive antenna at each user that maximizes the channel gain of the resulting *strong* user. To improve the user fairness, a new max-min-max antenna selection (AIA-AS) scheme is subsequently developed, in which we jointly select one transmit antenna at BS and corresponding best receive antennas at users to maximize the channel gain of the resulting *weak* user. For the CR-NOMA scenario, we propose another new antenna selection algorithm, termed maximum-channel-gain-based antenna selection (MCG-AS), to maximize the achievable rate of the secondary user, under the condition that the primary user's quality-of-service requirement is satisfied. The asymptotic closed-form expressions of the average sum-rate for A^3 -AS and AIA-AS and that of the average rate of the secondary user for MCG-AS are derived, respectively. Numerical results demonstrate that the AIA-AS provides better user-fairness, while the A^3 -AS achieves a near-optimal sum-rate in F-NOMA systems. For the CR-NOMA scenario, MCG-AS achieves a near-optimal performance in a wide signal-to-noise-ratio regime. Furthermore, all the proposed AS algorithms yield a significant computational complexity reduction, compared to exhaustive search-based counterparts.

Index Terms—Multiple-input multiple-output (MIMO), non-orthogonal multiple access (NOMA), antenna selection (AS).

I. INTRODUCTION

The non-orthogonal multiple access (NOMA) technique has emerged as a promising solution to significantly improve the spectral efficiency of the next-generation wireless networks [2]–[4]. By superimposing the information of multiple users in the power domain, multiple users can be served within the same time/frequency/code domain. Different from the conventional water-filling power allocation strategy, the NOMA technique generally allocates more transmit power to the users with the poor channel conditions (*weak* users). In this case, these users can decode their higher-power-level signals directly by treating others' signals as noise. In contrast, those users

with the better channel conditions (*strong* users) adopt the successive interference cancellation (SIC) technique for signal detection. It has been demonstrated that both the throughput performance and user fairness can be significantly improved in NOMA systems compared to conventional orthogonal multiple access (OMA) systems [2], [5].

Initial efforts on the design and analysis of the NOMA technique focused on single-antenna systems, see e.g., [6]–[12]. Recently, multiple antennas have been used in NOMA systems (MIMO-NOMA) to exploit the spatial degrees of freedom [13]–[17]. Although the system capacity can be potentially scaled up with the number of antennas, this superior performance comes at the price of expensive RF chains, high power consumption and computational complexity required for signal processing at both the transmitter and receivers. To avoid the high hardware costs, demanding power consumption and heavy computational burden while preserving the diversity and throughput benefits from MIMO, the antenna selection (AS) technique has been recognized as an effective solution [18]–[20]. There are only a few papers that considered the AS problem for MIMO-NOMA systems in the open literature. Specifically, a transmit AS (TAS) algorithm was proposed in [21], and a joint TAS and user scheduling algorithm was considered in [22]. However, both [21] and [22] only focused on the TAS design at the base station (BS) side and there were no analytical characterization of the system performance for the proposed algorithms.

To our best knowledge, joint AS at both the BS and users for MIMO-NOMA systems is still an open problem. Though there have been some published results on joint AS schemes in conventional MIMO-OMA systems, they cannot be extended to MIMO-NOMA systems directly. This is mainly because there is severe inter-user interference in MIMO-NOMA systems while the signals are transmitted in an interference-free manner in MIMO-OMA systems. A global optimal solution of this problem requires an exhaustive search (ES) over all possible antenna combinations, and its complexity would become unacceptable when the numbers of antennas at all terminals become large. Motivated by this, in this paper, we focus on the design and analysis of the low-complexity joint AS algorithms for a typical MIMO-NOMA downlink scenario, where a small number of users (e.g., two users) are grouped together to perform NOMA and different groups are admitted into the network in a OMA manner [2], [14], [23]. In particular, two commonly used power allocation policies: NOMA with fixed power allocation (F-NOMA) and NOMA with cognitive radio-inspired power allocation (CR-NOMA) [23]–[25], are considered respectively. In F-NOMA, the set

Y. Yu, H. Chen, Y. Li, and B. Vucetic are with the School of Electrical and Information Engineering, The University of Sydney, Sydney, NSW 2006, Australia (email: {yuehua.yu, he.chen, yonghui.li, branka.vucetic}@sydney.edu.au).

Z. Ding is with the School of Computing and Communications, Lancaster University, Lancaster LA1 4YW, U.K. (email: z.ding@lancaster.ac.uk).

L. Song is with the School of Electrical Engineering and Computer Science, Peking University, Beijing 100871, China (e-mail: lingyang.song@pku.edu.cn).

of power allocation coefficients is predefined and dynamically allocated to users in each resource block. In contrast, in CR-NOMA, the quality-of-service (QoS) requirements of users are satisfied with different priorities. Generally, the user with lower priority (i.e., secondary user, SU) is opportunistically served only when the QoS of user with higher priority (i.e., primary user, PU) is guaranteed. In this case, the set of power allocation coefficients in CR-NOMA is not predetermined but depending on the QoS requirement of the PU and the instantaneous channel order of users. Note that the design of low-complexity AS algorithm for MIMO-NOMA systems is fundamentally different from that for conventional MIMO-OMA systems. This is because multiple channel matrices with different distributions need to be considered concurrently to perform the antenna selection in NOMA, while only the channel status of one user is required for OMA. Furthermore, selecting different antenna not only affects the instantaneous channel gains of individual users, but also easily leads to different order of instantaneous channel gains of all users. This means that the information decoding order at the user side and the resulting expressions of the signal-to-interference-plus-noise (SINR) of different users are not predetermined but largely affected by the antenna selection process, which makes the design and analysis of antenna selection for MIMO-NOMA system non-trivial. The main contributions of this paper are summarized as follows:

- For the F-NOMA scenario, a max-max-max AS (A^3 -AS) algorithm is firstly designed to maximize the system sum-rate. This is achieved by selecting one antenna at the BS and corresponding best receive antenna at each user that maximize the channel gain of the resulting *strong* user. To improve the user fairness, a new max-min-max antenna selection (AIA-AS) scheme is subsequently developed, in which one transmit antenna at BS and corresponding best receive antennas at users are jointly selected to maximize the channel gain of the resulting *weak* user.
- For the CR-NOMA scenario, a joint antenna selection scheme called maximum-channel-gain-based AS (MCG-AS) algorithm is first proposed to maximize the achievable rate of the SU subject to the QoS requirements of the PU, and two simplified versions of MCG-AS, i.e., primary-user-based AS (PU-AS) and second-user-based AS (SU-AS), are subsequently presented to further reduce the computational complexity of MCG-AS.
- Asymptotic closed-form expressions for the average sum-rates (average rate of the SU) of the proposed algorithms in F-NOMA (CR-NOMA) systems are derived for high SNR scenarios, respectively.
- The computational complexities for all the proposed joint AS algorithms are considered, and are shown to be significantly lower than that of the ES-based schemes. Extensive simulation results illustrate that both A^3 -AS and AIA-AS in F-NOMA systems yield significant performance gains over the OMA ES-based scheme and the random selection scheme. In particular, A^3 -AS can achieve the near-optimal system sum-rate while AIA-AS can provide better user fairness. In CR-NOMA,

the MCG-AS scheme can achieve the near-optimal rate performance in a wide SNR regime. In contrast, the rate performance of both PU-AS and SU-AS is significantly affected by the distances between the BS and users. Specifically, the PU-AS (SU-AS) scheme can approach the optimal performance when the primary (secondary) user is closer to the BS.

The rest of the paper is organized as follows. In Section II, the considered MIMO-NOMA downlink model is introduced, and the joint AS optimization problems for both F-NOMA and CR-NOMA scenarios are formulated, respectively. In Section III, two new joint AS schemes for F-NOMA systems are proposed and their achievable sum-rate are analysed. In Section IV, a computationally-efficient joint AS algorithm and its two simplified versions are developed and analysed for CR-NOMA systems. Finally, simulation results and comparisons between the proposed algorithms and benchmark schemes are given in Section V, and conclusions are drawn in Section VI.

Notations: $\mathcal{C}^{m \times n}$ represents the set of all $m \times n$ matrices. All bold uppercase letters represent matrices, and all Calligraphic letters represent sets. $\Pr(\cdot)$ denotes the probability of an event, $\log(\cdot)$ denotes the logarithm function based on 2, and $|\cdot|$ and $\mathbb{E}[\cdot]$ denote the absolute value and the expectation operation, respectively. $F_X(x)$ and $f_X(x)$ represent the cumulative density function (CDF) and the probability density function (PDF) of a random variable X , respectively. \mathcal{O} is usually used in the efficiency analysis of algorithms and $q(x) = \mathcal{O}(p(x))$ when $\lim_{x \rightarrow \infty} \left| \frac{q(x)}{p(x)} \right| = c, 0 < c < \infty$.

II. SYSTEM MODEL

Consider a downlink communication scenario with one BS and multiple users. As discussed in [23], it is impractical to ask all the users in a system to perform NOMA due to the strong co-channel interference and heavy system overhead for user coordination. One promising alternative is to construct a hybrid multiple access system, wherein the users are divided into multiple small groups, and NOMA is implemented within each group while OMA is performed between different groups. Without loss of generality, in this paper, we follow [2], [14], [23] and assume two users¹ are paired in each group randomly to perform NOMA and different groups are admitted into the network in a time-division multiple access manner. There is no doubt that some other delicately designed user pairing schemes may further improve the rate performance of the NOMA implementation, however, it is out of the scope of this paper.

We consider that the BS is equipped with N antennas, while the two selected users (termed as UE_1 and UE_2) are equipped with M and K antennas, respectively. The channel matrix from the BS to UE_1 (UE_2) is denoted by $\mathbf{H} \in \mathcal{C}^{N \times M}$ ($\mathbf{G} \in \mathcal{C}^{N \times K}$). We assume that the channels between the BS and users undergo spatially independent flat Rayleigh fading. The entries of \mathbf{H} (\mathbf{G}), e.g., \tilde{h}_{nm} (\tilde{g}_{nk}), can be modelled as independent and identically distributed (i.i.d.) complex Gaussian random variables, where \tilde{h}_{nm} (\tilde{g}_{nk}) represents the channel coefficient between the n th antenna of the BS and the

¹Note that the two-user setting is how NOMA is implemented in LTE-Advanced.

m th (k th) antenna of UE₁ (UE₂). For notation simplicity, we define $h_{nm} = |\tilde{h}_{nm}|^2$ and $g_{nk} = |\tilde{g}_{nk}|^2$.

As in [26], [27], we assume that the BS selects one (e.g., n th) out of N available antennas to transmit information, while the users select one (e.g., m th and k th) out of M and K available antennas to receive messages, respectively. In this case, only one RF chain is needed at each node such that the hardware cost and complexity can be reduced. Moreover, only the partial channel state information (CSI), i.e., the channel amplitudes, is needed instead of the full CSI at the BS, which costs much less feedback bandwidth².

Let $\delta_{n,m,k}$ denote the channel order indicator, defined as

$$\delta_{n,m,k} = \begin{cases} 1, & \text{if } h_{nm} \geq g_{nk}, \\ 0, & \text{if } h_{nm} < g_{nk}. \end{cases} \quad (1)$$

According to the NOMA principle, the BS broadcasts the signals superimposed in the power domain as

$$x = \delta_{n,m,k}(\sqrt{b}s_1 + \sqrt{a}s_2) + (1 - \delta_{n,m,k})(\sqrt{a}s_1 + \sqrt{b}s_2), \quad (2)$$

where s_i denotes the signal to UE _{i} with $\mathbb{E}[|s_i|^2] = 1$, and a and b are the power allocation coefficients with $a + b = 1$. Without loss of generality, we assume that $a > b$ to guarantee that more power is allocated to the instantaneous *weak* user.

The received signals at users are given by

$$y_1 = \sqrt{P_s}\tilde{h}_{nm}x + n_1, \quad y_2 = \sqrt{P_s}\tilde{g}_{nk}x + n_2, \quad (3)$$

where P_s is the transmit power at the BS, and n_i is the complex additive white Gaussian noise with variance σ_i^2 . For notational simplicity, we hereafter assume $\sigma_1^2 = \sigma_2^2 = \sigma^2$.

When $\delta_{n,m,k} = 1$, UE₂ is the *weak* user and UE₁ is the *strong* user, hence the power level of s_2 is larger than that of s_1 . In this case, UE₂ decodes s_2 directly by treating s_1 as noise. In contrast, UE₁ first decodes s_2 and subtracts it via SIC, and then decodes its own s_1 without interference. For the case $\delta_{n,m,k} = 0$, the decoding order is reversed. By using the fact that the channels are ordered, it can be easily verified that SIC can be implemented successfully, and the following two rates can be achievable to UE₁ and UE₂, respectively:

$$R_1 = \delta_{n,m,k} \log(1 + \rho b h_{nm}) + (1 - \delta_{n,m,k}) \log\left(1 + \frac{a h_{nm}}{b h_{nm} + \frac{1}{\rho}}\right), \quad (4)$$

$$R_2 = \delta_{n,m,k} \log\left(1 + \frac{a g_{nk}}{b g_{nk} + \frac{1}{\rho}}\right) + (1 - \delta_{n,m,k}) \log(1 + \rho b g_{nk}), \quad (5)$$

where $\rho = P_s/\sigma^2$ is the transmit SNR.

To evaluate the user fairness, the Jain's fairness index [28] is adopted in this paper, which can be expressed as

$$\eta = (R_1 + R_2)^2 / 2(R_1^2 + R_2^2). \quad (6)$$

We can observe that the Jain's fairness index is bounded between 0 and 1 with the maximum achieved by equalling

²It is worth noting that for the case of slow fading (i.e., the channel coherent time is long such that the time used for channel estimation can be neglected compared to the duration of each transmission block), the obtained results in this paper can serve as a tight performance bound for the case of considering channel estimation overhead. When the channels change relatively quickly, the impact of channel estimation overhead can be significant. However, incorporating the channel estimation cost into the considered MIMO-NOMA system will require the definition of new system performance metric, the joint optimization of channel estimation overhead, antenna selection, and power allocation, which could constitute a new full paper and thus has been left as a future work.

user's rates. Note that the Jain's fairness index is a performance metric rather than an approach to guarantee the fairness of the considered MIMO-NOMA systems. To improve user fairness, the interested readers are referred to various power allocation schemes for NOMA, e.g., ordered power allocation [29], max-min power allocation [30], and α -fairness [31], etc.

In the following subsections we formulate the joint AS optimization problems for two MIMO-NOMA scenarios, i.e., F-NOMA and CR-NOMA, respectively.

A. Joint AS Optimization Problem for F-NOMA Systems

In F-NOMA, fixed power allocation coefficients are predefined. In this case, we can formulate the following optimization problem to maximize the achievable system sum-rate

$$\mathbf{P1}: \{n^*, m^*, k^*\} = \arg \max_{n \in \mathcal{N}, m \in \mathcal{M}, k \in \mathcal{K}} R_{\text{sum}}(h_{nm}, g_{nk}), \quad (7)$$

where $\mathcal{N} = \{1, 2, \dots, N\}$, $\mathcal{M} = \{1, 2, \dots, M\}$, $\mathcal{K} = \{1, 2, \dots, K\}$ and the achievable sum-rate is given by

$$\begin{aligned} R_{\text{sum}}(h_{nm}, g_{nk}) &= R_1 + R_2 \\ &= \log(1 + \rho b \gamma_n^s) + \log\left(1 + \frac{a \gamma_n^w}{b \gamma_n^w + 1/\rho}\right), \end{aligned} \quad (8)$$

where $\gamma_n^s = \max(h_{nm}, g_{nk})$ denotes the channel gain of the *strong* user and $\gamma_n^w = \min(h_{nm}, g_{nk})$ denotes the channel gain of the *weak* user. It is worth pointing out that for a given time slot, which user is the *strong* (*weak*) user is not predefined, but depending on the channel fluctuations and antenna selection result. This uncertainty needs to be carefully considered when designing the antenna selection algorithm.

B. Joint AS Optimization for CR-NOMA Systems

In the considered CR-NOMA downlink scenario, without loss of generality, we treat UE₂ as the primary user and UE₁ as the secondary user. Specifically, UE₁ is opportunistically served when the QoS of UE₂ is achieved. Hereafter we use R_1^c and R_2^c to respectively denote the achievable rate of UE₁ and UE₂, where the superscript $(\cdot)^c$ is used to distinguish the parameters in CR-NOMA systems from those in F-NOMA systems. Mathematically, the achievable rate of the secondary user, R_2^c , should satisfy $R_2^c \geq R_{\text{th}}$, where R_{th} is the QoS threshold of UE₂. By noting that the power allocation coefficient $0 \leq b_{n,m,k}^c \leq 1$, we can express the valid range of $b_{n,m,k}^c$ as below:

$$b_{n,m,k}^c = \begin{cases} \min\left(\frac{\varepsilon}{\rho g_{nk}}, 1\right), & \text{if } \delta_{n,m,k} = 0, \\ \max\left(\frac{\rho g_{nk} - \varepsilon}{\rho g_{nk}(\varepsilon + 1)}, 0\right), & \text{if } \delta_{n,m,k} = 1, \end{cases} \quad (9)$$

where $\varepsilon = 2^{R_{\text{th}}} - 1$, and we then have $a_{n,m,k}^c = 1 - b_{n,m,k}^c$.

By substituting (9) into (4), we can observe that the achievable rate of the secondary user, R_1^c , is zero when $\delta_{n,m,k} = 0$, $b_{n,m,k}^c = 1$ or $\delta_{n,m,k} = 1$, $b_{n,m,k}^c = 0$. In other words, when the QoS of UE₂ cannot be satisfied, no power would be allocated to UE₁ and hence $R_1^c = 0$. For the considered high SNR scenarios, i.e., $\rho \rightarrow \infty$, the expression of $b_{n,m,k}^c$ given in (9) can be simplified as

$$b_{n,m,k}^c = \begin{cases} \frac{\varepsilon}{\rho g_{nk}}, & \text{if } \delta_{n,m,k} = 0, \\ \frac{\rho g_{nk} - \varepsilon}{\rho g_{nk}(\varepsilon + 1)}, & \text{if } \delta_{n,m,k} = 1. \end{cases} \quad (10)$$

By substituting (10) into (4), the achievable rate of the secondary user (i.e., R_1^c) can be represented as

$$\begin{aligned} R_1^c(h_{nm}, g_{nk}) &= \delta_{n,m,k} \log\left(1 - \frac{\varepsilon h_{nm}}{(\varepsilon+1)g_{nk}} + \frac{\rho h_{nm}}{\varepsilon+1}\right) \\ &+ (1 - \delta_{n,m,k}) \log\left(\frac{g_{nk}}{\varepsilon h_{nm} + g_{nk}} + \frac{\rho h_{nm} g_{nk}}{\varepsilon h_{nm} + g_{nk}}\right) \\ &\stackrel{\rho \rightarrow \infty}{\approx} \delta_{n,m,k} \log\left(\frac{\rho h_{nm}}{\varepsilon+1}\right) \\ &+ (1 - \delta_{n,m,k}) \log\left(\frac{\rho h_{nm} g_{nk}}{\varepsilon h_{nm} + g_{nk}}\right). \end{aligned} \quad (11)$$

Now we can formulate the following joint AS problem for CR-NOMA systems:

$$\begin{aligned} \mathbf{P2} : \{n^*, m^*, k^*\} &= \arg \max_{n \in \mathcal{N}, m \in \mathcal{M}, k \in \mathcal{K}} R_1^c(h_{nm}, g_{nk}) \\ \text{s.t. } R_2^c(h_{nm}, g_{nk}) &\geq R_{\text{th}}. \end{aligned} \quad (12)$$

It is straightforward to see that both **P1** and **P2** are NP-hard problems, which mean finding the optimal combinations of antennas at both the BS and users may require an exhaustive search with the complexity of $\mathcal{O}(NMK)$. This becomes unaffordable when N , M and K become large. Motivated by this, in the subsequent two sections we will develop joint AS algorithms for F-NOMA and CR-NOMA systems with significantly reduced computational complexity, respectively.

III. ANTENNA SELECTION FOR F-NOMA SYSTEMS

In this section, two low-complexity joint AS algorithms are developed to maximize the system sum-rate for F-NOMA systems without and with the consideration of user fairness. The closed-form expressions for the average sum-rate of these two proposed algorithms are derived in high SNR regime.

A. Proposed AS Algorithms for F-NOMA Systems

We can readily verify that the sum-rate R_{sum} defined in (8) is a monotonically increasing function of the channel gains of both the *strong* and *weak* user (i.e., γ_n^s and γ_n^w). Unfortunately, γ_n^s and γ_n^w cannot be maximized at the same time in most cases. This is because both the two users need to share the same transmit antenna of the BS and it is very less likely that selecting one of the transmit antennas can lead to the maximum channel gains of both users. Based on this observation, we propose two new joint AS schemes for the considered F-NOMA systems in this subsection, termed max-max-max AS (A^3 -AS) and max-min-max AS (AIA-AS), respectively. The key idea of A^3 -AS (AIA-AS) is to make γ_n^w (γ_n^s) as large as possible under the condition that γ_n^s (γ_n^w) is maximized. More details are elaborated as below.

1) A^3 -AS: A^3 -AS mainly consists of three stages.

- **Stage 1.** For a given transmit antenna, we firstly find the best receive antennas for UE₁ and UE₂, respectively. Mathematically, we need to find out the largest element h_n^{\max} (g_n^{\max}) in each row of \mathbf{H} (\mathbf{G}) as follows:

$$h_n^{\max} = \max(h_{n1}, \dots, h_{nM}), \quad (13)$$

$$g_n^{\max} = \max(g_{n1}, \dots, g_{nK}), \quad (14)$$

for $n \in \mathcal{N}$. Each pair (h_n^{\max}, g_n^{\max}) is then treated as one AS candidate. The set of all the N pairs can be written as $\mathcal{S}_{A^3}^{(1)} = \{(h_1^{\max}, g_1^{\max}), \dots, (h_N^{\max}, g_N^{\max})\}$.

- **Stage 2.** For a given pair from $\mathcal{S}_{A^3}^{(1)}$, the one with larger channel gain is set as the *strong* user while the other one is set as the *weak* user. In order to maximize the channel gain of the *strong* user, we need to find out all its potential channel gains. Mathematically, we need to find out the *larger* element of (h_n^{\max}, g_n^{\max}) as follows:

$$\gamma_n^s = \max(h_n^{\max}, g_n^{\max}), \quad n \in \mathcal{N}. \quad (15)$$

The set of the N *larger* elements are denoted by $\mathcal{S}_{A^3}^{(2)} = \{\gamma_1^s, \dots, \gamma_N^s\}$.

- **Stage 3.** After obtaining the set of the potential channel gains of the *strong* user, we thirdly find out the largest one from $\mathcal{S}_{A^3}^{(2)}$ to maximize γ_n^s . Mathematically, we have

$$\gamma_{A^3}^s = \max(\gamma_n^s), \quad n \in \mathcal{N}. \quad (16)$$

Recall that $\gamma_{A^3}^s$ coming from UE₁ or UE₂ is not predetermined, we then use $(n_{A^3}^*, m_{A^3}^*)$ to denote the original row and column indexes of $\gamma_{A^3}^s$ when it lies in \mathbf{H} . In this case, the $n_{A^3}^*$ th antenna at the BS and the $m_{A^3}^*$ th antenna at UE₁ are selected. We use $k_{A^3}^*$ to denote the original column index of $\gamma_{A^3}^w = g_{n_{A^3}^*}^{\max}$. Therefore the $k_{A^3}^*$ th antenna at UE₂ can be selected concurrently. For the case that $\gamma_{A^3}^s$ lies in \mathbf{G} , the selected antenna indexes can be obtained in a similar way.

In A^3 -AS, the channel gain of the instantaneous *strong* user $\gamma_{A^3}^s$ is maximized. However, the achievable rate of the instantaneous *weak* user cannot be guaranteed and may be worse for some cases. Recall that the Jain's fairness index decreases when the gap between the achievable rates of users enlarges. In order to improve the user fairness, we subsequently develop a AIA-AS scheme, which aims to improve the rate performance of the instantaneous *weak* user and to narrow the gap of the rates of users.

2) AIA-AS: Similar to the A^3 -AS algorithm, the AIA-AS scheme also has three stages. The main difference between A^3 -AS and AIA-AS lies in the second and the third stages. In particular, A^3 -AS constructs the set of all potential channel gains for the *strong* user and then maximizes γ_n^s . In contrast, AIA-AS tries to obtain the set of all potential channel gains for the *weak* user and then to maximize γ_n^w . The three stages of AIA-AS are elaborated as follow.

- **Stage 1.** Construct the set $\mathcal{S}_{AIA}^{(1)} = \{(h_1^{\max}, g_1^{\max}), \dots, (h_N^{\max}, g_N^{\max})\}$ as (13) and (14).
- **Stage 2.** In order to maximize the channel gain of the *weak* user, we need to find out all the potential channel gains of the *weak* user from $\mathcal{S}_{AIA}^{(1)}$. Mathematically, we need to find out the *smaller* element in each pair of (h_n^{\max}, g_n^{\max}) , that is,

$$\gamma_n^w = \min(h_n^{\max}, g_n^{\max}), \quad n \in \mathcal{N}. \quad (17)$$

The set containing these N smaller elements is denoted by $\mathcal{S}_{AIA}^{(2)} = \{\gamma_1^w, \dots, \gamma_N^w\}$.

- **Stage 3.** After obtaining the set of the potential channel gains of the *weak* user, we thirdly find out the largest one from $\mathcal{S}_{AIA}^{(2)}$ to maximize γ_n^w . Mathematically, we have

$$\gamma_{AIA}^w = \max(\gamma_n^w), \quad n \in \mathcal{N}. \quad (18)$$

Similarly, we can see that γ_{AIA}^w coming from UE₁ or UE₂ is not predefined. We use (n_{AIA}^*, k_{AIA}^*) to denote the original row and column indexes of γ_{AIA}^w when it lies in \mathbf{G} . In this case, the n_{AIA}^* th antenna at the BS and the k_{AIA}^* th antenna at UE₂ are selected, respectively. Meanwhile, we use m_{AIA}^* to denote the original column index of $\gamma_{AIA}^s = h_{n_{AIA}^*}^{\max}$. Therefore the m_{AIA}^* th antenna at UE₁ can be selected simultaneously. For the case that γ_{AIA}^w lies in \mathbf{H} , the selected antenna indexes can be obtained in a similar way.

3) *Computational Complexities Comparisons*: As mentioned before, the complexity of the optimal selection algorithm achieved by the ES-based scheme in F-NOMA systems is as high as $\mathcal{O}(NMK)$. When the number of antennas at each node becomes large, e.g., up to hundreds of antennas [32], the computational burden would increase significantly.

The two new AS algorithms for F-NOMA systems dramatically reduce the selection complexity to $\mathcal{O}(N(M+K+3))$, where the main computation lies in sorting the channel gains. For the case $N = M = K$, we can find that the complexities of A³-AS and AIA-AS are approximately $\mathcal{O}(N^2)$, which is an order of magnitude lower compared to that of the optimal ES scheme, which is $\mathcal{O}(N^3)$.

B. Performance Analysis of the New Algorithms for F-NOMA

In this subsection, we analyse the average sum-rate of the proposed joint AS algorithms, i.e., A³-AS and AIA-AS in F-NOMA systems, respectively.

Assuming flat Rayleigh fading, h_{nm} is then an exponentially distributed random variable. When $x \geq 0$, the CDF and PDF of h_{nm} are respectively given by

$$F_h(x) = 1 - e^{-\Omega_h x}, \quad f_h(x) = \Omega_h e^{-\Omega_h x}, \quad (19)$$

where $\Omega_h = 1/\mathbb{E}[h_{nm}]$. Similarly, when $x \geq 0$ we have the CDF and PDF of g_{nk} as follows,

$$F_g(x) = 1 - e^{-\Omega_g x}, \quad f_g(x) = \Omega_g e^{-\Omega_g x}, \quad (20)$$

where $\Omega_g = 1/\mathbb{E}[g_{nk}]$.

Recall that both the two proposed AS schemes for F-NOMA need to find the maximum element in each row of \mathbf{H} and \mathbf{G} (i.e., h_n^{\max} and g_n^{\max}). We thus first obtain the distribution functions of h_n^{\max} for $x \geq 0$ as below,

$$F_{h_n^{\max}}(x) = (1 - e^{-\Omega_h x})^M \stackrel{(c_1)}{=} \sum_{i=0}^M \mu_{i,M} e^{-i\Omega_h x}, \quad (21)$$

$$f_{h_n^{\max}}(x) = -\sum_{i=1}^M i\Omega_h \mu_{i,M} e^{-i\Omega_h x}, \quad (22)$$

where $\mu_{i,M} = (-1)^i \binom{M}{i}$ and the expansion step (c_1) is conducted based on the Binomial theorem.

Similarly, the CDF and PDF of g_n^{\max} for $x \geq 0$ are given by

$$F_{g_n^{\max}}(x) = (1 - e^{-\Omega_g x})^K = \sum_{j=0}^K \mu_{j,K} e^{-j\Omega_g x}, \quad (23)$$

$$f_{g_n^{\max}}(x) = -\sum_{j=1}^K j\Omega_g \mu_{j,K} e^{-j\Omega_g x}. \quad (24)$$

From the sum-rate expression of the considered F-NOMA system in (8), we can observe that the achievable rate of the instantaneous *weak* UE approaches a constant when $\rho \rightarrow \infty$, i.e., $\log\left(1 + \frac{a\gamma_n^w}{b\gamma_n^w + 1/\rho}\right) \stackrel{\rho \rightarrow \infty}{\approx} \log\left(1 + \frac{a}{b}\right) = \log(1/b)$ with $a + b = 1$, which is only related to the predefined power

allocation coefficient b . In this case, we mainly focus on the contribution of the instantaneous *strong* user to the sum-rate. Mathematically, we have the approximation of the system instantaneous sum-rate given in (8) as follows:

$$R_{\text{sum}}(\gamma_n^s) \stackrel{\rho \rightarrow \infty}{\approx} \log(1 + b\rho\gamma_n^s) + \log(1/b). \quad (25)$$

Subsequently, we perform the asymptotic analysis for the average sum-rates of A³-AS and AIA-AS algorithms, respectively.

1) *Average Sum-Rate Analysis for A³-AS*: Let $h^{\max} = \max(h_{nk})$ and $g^{\max} = \max(g_{nk})$ for $n \in \mathcal{N}$, $m \in \mathcal{M}$ and $k \in \mathcal{K}$. Recall that in A³-AS, $\gamma_{A^3}^s$ is actually the relatively larger element of h^{\max} and g^{\max} . In order to obtain the distribution of $\gamma_{A^3}^s$, at first we derive the CDF and PDF of h^{\max} and g^{\max} respectively as follows:

$$F_{h^{\max}}(x) = \sum_{i=0}^{NM} \mu_{i,NM} e^{-i\Omega_h x}, \quad (26)$$

$$f_{h^{\max}}(x) = -\sum_{i=1}^{NM} i\Omega_h \mu_{i,NM} e^{-i\Omega_h x}, \quad (27)$$

$$F_{g^{\max}}(x) = \sum_{j=0}^{NK} \mu_{j,NK} e^{-j\Omega_g x}, \quad (28)$$

$$f_{g^{\max}}(x) = -\sum_{j=1}^{NK} j\Omega_g \mu_{j,NK} e^{-j\Omega_g x}. \quad (29)$$

Then the CDF and PDF of $\gamma_{A^3}^s = \max(h^{\max}, g^{\max})$ in A³-AS can be calculated as follows

$$\begin{aligned} F_{\gamma_{A^3}^s}(x) &= \Pr(\max(h^{\max}, g^{\max}) < x) \\ &= \Pr(h^{\max} \leq g^{\max} < x) + \Pr(g^{\max} < h^{\max} < x), \quad (30) \\ f_{\gamma_{A^3}^s}(x) &= f_{g^{\max}}(x) \int_0^x f_{h^{\max}}(y) dy + f_{h^{\max}}(x) \int_0^x f_{g^{\max}}(y) dy \\ &= \sum_{i=1}^{NM} \sum_{j=1}^{NK} \mu_{i,NM} \mu_{j,NK} (i\Omega_h e^{-i\Omega_h x} \\ &\quad + j\Omega_g e^{-j\Omega_g x} - (i\Omega_h + j\Omega_g) e^{-(i\Omega_h + j\Omega_g)x}). \quad (31) \end{aligned}$$

We now can analyse the average sum-rate of A³-AS for high SNR scenarios and obtain Proposition 1 as below.

Proposition 1. *With the PDF of $\gamma_{A^3}^s$ in A³-AS, i.e., $f_{\gamma_{A^3}^s}(x)$, when $\rho \rightarrow \infty$, the asymptotic closed-form expression for the average sum-rate of the A³-AS algorithm is given by*

$$\begin{aligned} \bar{R}_{\text{sum}}^{A^3} &\approx \frac{1}{\ln 2} (\ln \rho - C) \\ &\quad + \sum_{i=1}^{NM} \sum_{j=1}^{NK} \frac{(-1)^{i+j} \binom{NM}{i} \binom{NK}{j}}{\ln 2} \ln \left(\frac{i\Omega_h + j\Omega_g}{ij\Omega_h\Omega_g} \right) \quad (32) \end{aligned}$$

Proof: See Appendix A. ■

As can be observed from (32), the system sum-rate $\bar{R}_{\text{sum}}^{A^3}$ is an increasing function of the transmit SNR ρ as expected. Interestingly, it is not affected by the power allocation coefficient b . The reason behind this observation is that when $\rho \rightarrow \infty$, $R_{\text{sum}} \approx \log(\gamma^s \rho)$, in which the power allocation factor b has been removed. It will be verified via the computer simulations in section V.

2) *Average Sum-rate Analysis for AIA-AS*: In this subsection, we derive the asymptotic average sum-rate of the proposed AIA-AS algorithm, i.e., $\bar{R}_{\text{sum}}^{AIA}$, for high SNR scenarios. According to (25), we need to know the PDF of the channel gain of the instantaneous *strong* user who shares the transmit antenna with the *weak* user, i.e., $f_{\gamma_{AIA}^s}(x)$. With the help of

the law of full probability and the multinomial theorem, the PDF of $f_{\gamma_{AIA}^s}(x)$ is provided in Lemma 1 as below.

Lemma 1. *In the AIA-AS algorithm, the PDF of the channel gain of the selected strong user, i.e., γ_{AIA}^s , is given by*

$$f_{\gamma_{AIA}^s}(x) = \sum_{i=1}^M \sum_{j=1}^K \sum_{\ell} C_{\ell} t_{\ell} \zeta_{ij} (\psi(i\Omega_h, j\Omega_g) + \psi(j\Omega_g, i\Omega_h)), \quad (33)$$

where

$$\begin{aligned} C_{\ell} &= \frac{(N-1)!}{\ell_0! \cdots \ell_{MK}!} \text{ for } \ell_0 + \cdots + \ell_{MK} = N-1, \\ t_{\ell} &= \prod_{\substack{1 \leq i \leq M \\ 1 \leq j \leq K}} (-\mu_{i,M} \mu_{j,K})^{\ell_{ij}}, \\ \zeta_{ij} &= N i j \Omega_h \Omega_g \mu_{i,M} \mu_{j,K}, \\ \psi(\theta_1, \theta_2) &= e^{-\theta_1 x} \left(\frac{e^{-\theta_2 x} - 1}{\theta_2} - \frac{e^{-(\theta_2 + \xi_{\ell})x} - 1}{\theta_2 + \xi_{\ell}} \right), \\ \xi_{\ell} &= \sum_{i=1}^M \sum_{j=1}^K (i\Omega_h + j\Omega_g) \ell_{ij}. \end{aligned}$$

Proof: See Appendix B. \blacksquare

Provided the PDF of γ_{AIA}^s in AIA-AS algorithm, we can approximate the average sum-rate achieved by AIA-AS in Proposition 2 as below.

Proposition 2. *With the PDF of γ_{AIA}^s , when $\rho \rightarrow \infty$, the asymptotic average sum-rate of AIA-AS, i.e., $\bar{R}_{\text{sum}}^{AIA}$, is given by*

$$\bar{R}_{\text{sum}}^{AIA} \approx \log \frac{1}{b} + \sum_{i=1}^M \sum_{j=1}^K \sum_{\ell} \frac{C_{\ell} t_{\ell}}{\ln 2} (T_1 + T_2 + T_3 + T_4), \quad (34)$$

where T_n , $n = \{1, 2, 3, 4\}$ are given by

$$\begin{aligned} T_1 &= \frac{\xi_{\ell} \tilde{\zeta}_{ij}}{\phi_i} \chi(j\Omega_g), \quad T_2 = \frac{\xi_{\ell} \tilde{\zeta}_{ij}}{\phi_j} \chi(i\Omega_h), \\ T_3 &= \frac{\zeta_{ij} \phi_{ij,2} \chi(\phi_{ij,1})}{\phi_i \phi_j \phi_{ij,1}}, \quad T_4 = -\tilde{\zeta}_{ij} \chi(i\Omega_h + j\Omega_g), \end{aligned}$$

in which, $\tilde{\zeta}_{ij} = N \mu_{i,M} \mu_{j,K}$, $\phi_i = i\Omega_h + \xi_{\ell}$, $\phi_j = j\Omega_g + \xi_{\ell}$, $\phi_{ij,1} = i\Omega_h + j\Omega_g + \xi_{\ell}$, $\phi_{ij,2} = i\Omega_h + j\Omega_g + 2\xi_{\ell}$, $\chi(x) = C + \ln \frac{x}{b\rho}$, and the constant C is the Euler's constant.

Proof: See Appendix C. \blacksquare

IV. ANTENNA SELECTION FOR CR-NOMA SYSTEMS

In this section, CR-NOMA is considered, and a computationally efficient joint AS algorithm, i.e., MCG-AS, is proposed to maximize the achievable rate of secondary user UE₁. To further reduce the computational complexity, two simplified versions of MCG-AS, i.e., PU-AS and SU-AS, are proposed. In the high SNR regime, the asymptotic expressions of average achievable rates of UE₁ using MCG-AS, PU-AS and SU-AS are then derived, respectively.

A. Proposed AS Algorithms for CR-NOMA Systems

By observing (9)-(11), we can see that the channel gain of the primary user UE₂ (i.e., g_{nk}) and that of the secondary user UE₁ (i.e., h_{nm}) both make contributions to R_1^c but in different ways in CR-NOMA systems. In particular, if g_{nk} increases, less power would be needed to satisfy the QoS requirement of UE₂. In other words, more power can be allocated to UE₁ and

hence R_1^c increases. In contrast, the contribution of h_{nm} to R_1^c does not lie in the power domain, but can boost R_1^c directly via providing a better channel gain. However, it is not easy to tell which one, g_{nk} or h_{nm} , has greater contribution to R_1^c . In this case, we propose to maximize the contribution of the larger one from g_{nk} and h_{nm} . Accordingly, a low-complexity AS algorithm, referred to as MCG-AS, is developed for the considered CR-NOMA system. More specifically, the MCG-AS algorithm consists of four stages as below.

- **Stage 1.** Find out the best transmit and receive candidates for UE₁ (UE₂) which can maximize h_{nm} (g_{nk}). Mathematically, we have

$$h^{\max} = \max(h_{n1}, \cdots, h_{NM}), \quad (35)$$

$$g^{\max} = \max(g_{n1}, \cdots, g_{NK}). \quad (36)$$

- **Stage 2.** Compare and find out the larger one from h^{\max} and g^{\max} and set it as the channel gain of the *strong* user. That is,

$$\gamma_{\text{MCG}}^s = \max(h^{\max}, g^{\max}). \quad (37)$$

Denote the row index of γ_{MCG}^s as n_{MCG}^* . Then, the n_{MCG}^* th antenna at the BS can be selected.

- **Stage 3.** Since the *weak* user share the same transmit antenna with the *strong* user, we should find out the largest element γ_{MCG}^w for the *weak* user from the same n_{MCG}^* th row. Mathematically, we have

$$\gamma_{\text{MCG}}^w = \begin{cases} \max(g_{n_{\text{MCG}}^*1}, \cdots, g_{n_{\text{MCG}}^*K}), & \text{if } \gamma_{\text{MCG}}^s = h^{\max}, \\ \max(h_{n_{\text{MCG}}^*1}, \cdots, h_{n_{\text{MCG}}^*M}), & \text{if } \gamma_{\text{MCG}}^s = g^{\max}. \end{cases} \quad (38)$$

For the case that $\gamma_{\text{MCG}}^s = h^{\max}$, we denote the original column indexes of γ_{MCG}^s and γ_{MCG}^w as m_{MCG}^* and k_{MCG}^* , respectively. Then, the m_{MCG}^* th antenna at UE₁ and the k_{MCG}^* th antenna at UE₂ can be selected concurrently. For the case that $\gamma_{\text{MCG}}^s = g^{\max}$, the corresponding antenna indexes at users can be obtained similarly.

- **Stage 4.** Compute b_{n^*, m^*, k^*}^c and a_{n^*, m^*, k^*}^c by substituting γ_{MCG}^s and γ_{MCG}^w to (10).

We also realize that, when the primary user UE₂ is much closer to the BS than the secondary user UE₁, it is likely that g^{\max} is larger than h^{\max} . In this case, MCG-AS can be simplified into the PU-AS scheme, in which the AS can be performed by maximizing the channel gain of the primary user UE₂. In this sense, more power can be allocated to the secondary user UE₁. In contrast, when UE₂ is much farther from the BS than UE₁, it is likely that g^{\max} is smaller than h^{\max} . In this case, MCG-AS can be reduced to the SU-AS scheme, which aims to maximize the channel gain of the secondary user UE₁ directly. We elaborate the principles and key stages of the simplified PU-AS and SU-AS in the subsequent two subsections.

1) *PU-AS:* The key idea of PU-AS is to select the antenna pair from the BS and the primary user UE₂ concurrently, which provides the maximum channel gain for UE₂. In this case, less power is needed for UE₂ to satisfy its QoS requirement and more power can thus be allocated to the secondary user UE₁ to increase the corresponding R_1^c . The main three stages of PU-AS scheme are described as below.

TABLE I: Complexity comparison in CR-NOMA

	Computational Complexity
CR-NOMA-ES	$\mathcal{O}(NMK)$
MCG-AS	$\mathcal{O}(N(M+K)+2)$
PU-AS	$\mathcal{O}(NK+M)$
SU-AS	$\mathcal{O}(NM+K)$

- **Stage 1.** Find out the best transmit and receive antennas for UE₂ to maximize its channel gain. Mathematically, that is to find out the largest element g^{\max} from \mathbf{G} ,

$$g^{\max} = \max(g_{i1}, \dots, g_{NK}). \quad (39)$$

Denote the row and column indexes of g^{\max} as n_p^* and k_p^* , respectively. Then, the n_p^* th antenna at the BS and the k_p^* th antenna at UE₂ are selected simultaneously.

- **Stage 2.** For the n_p^* th selected transmit antenna, find out the best receive antenna for UE₁ who shares the same transmit antenna with UE₂. Mathematically, find out the largest element $h_{n_p^*}^{\max}$ in the n_p^* th row of \mathbf{H} . That is,

$$h_{n_p^*}^{\max} = \max(h_{n_p^*1}, \dots, h_{n_p^*M}). \quad (40)$$

Denote the column index of $h_{n_p^*}^{\max}$ as m_p^* . Then, the m_p^* th antenna at UE₁ is selected.

- **Stage 3.** Calculate $b_{n_p^*, m_p^*, k_p^*}^c$ and $a_{n_p^*, m_p^*, k_p^*}^c$ by substituting the value of g^{\max} and $h_{n_p^*}^{\max}$ to (10).

2) *SU-AS*: The key idea of SU-AS is to first select the antenna pair from the BS and secondary user UE₁ concurrently, which provides the maximum channel gain for UE₁. Similarly, SU-AS consists of three stages.

- **Stage 1.** Find out the largest element h^{\max} from \mathbf{H} .

$$h^{\max} = \max(h_{i1}, \dots, h_{NM}). \quad (41)$$

Denote the row and column indexes of h^{\max} as n_s^* and m_s^* , respectively. Then, the n_s^* th antenna at the BS and the m_s^* th antenna at UE₁ are selected simultaneously.

- **Stage 2.** Find out the largest element $g_{n_s^*}^{\max}$ in the n_s^* th row of \mathbf{G} . Mathematically,

$$g_{n_s^*}^{\max} = \max(g_{n_s^*1}, \dots, g_{n_s^*K}). \quad (42)$$

Denote the column index of $g_{n_s^*}^{\max}$ as k_s^* . Then, the k_s^* th antenna at UE₂ is selected.

- **Stage 3.** Obtain $b_{n_s^*, m_s^*, k_s^*}^c$ and $a_{n_s^*, m_s^*, k_s^*}^c$ by substituting the value of h^{\max} and $g_{n_s^*}^{\max}$ to (10).

3) *Computational Complexities Comparisons*: Similar to F-NOMA systems, the complexity of the optimal selection algorithm achieved by the ES-based scheme in CR-NOMA systems is also as high as $\mathcal{O}(NMK)$. In contrast, all the three proposed AS algorithms, i.e., MCG-AS, PU-AS and SU-AS, can dramatically reduce the selection complexities as illustrated in Table I. Furthermore, the complexities of PU-AS and SU-AS are lower than that of MCG-AS. For the case $N=M=K$, the computational burdens of PU-AS and SU-AS are nearly half of that of MCG-AS.

B. Average Rate Analysis of the SU in CR-NOMA

As discussed above, since the QoS of the primary user UE₂ is guaranteed in CR-NOMA systems, we thus only focus on the analysis of the average rate of the secondary user UE₁, which is served opportunistically in CR-NOMA networks.

For the proposed MCG-AS scheme, by carefully analysing its antenna selection procedure, we can find that the MCG-AS scheme would become SU-AS when $h^{\max} \geq g^{\max}$ and would simplify to PU-AS otherwise. In this case, the average rate of UE₁ in MCG-AS (i.e., \bar{R}_1^{MCG}) can be calculated according to the law of total probability as below:

$$\bar{R}_1^{\text{MCG}} = \Pr(h^{\max} < g^{\max}) \bar{R}_1^{\text{P}} + \Pr(h^{\max} \geq g^{\max}) \bar{R}_1^{\text{S}}, \quad (43)$$

where \bar{R}_1^{P} and \bar{R}_1^{S} denote the average rate of UE₁ in PU-AS and SU-AS, respectively, and the probability of the event that $h^{\max} \geq g^{\max}$ is given by

$$\begin{aligned} \Pr(h^{\max} \geq g^{\max}) &= \int_0^\infty f_{h^{\max}}(x) \int_0^x f_{g^{\max}}(y) dy dx \\ &= \sum_{i=1}^{NM} \sum_{j=1}^{NK} \frac{(-1)^{i+j} \binom{NM}{i} \binom{NK}{j} j \Omega_g}{i \Omega_h + j \Omega_g}. \end{aligned} \quad (44)$$

Accordingly, $\Pr(h^{\max} < g^{\max}) = 1 - \Pr(h^{\max} \geq g^{\max})$. Therefore, the analytical expression of \bar{R}_1^{MCG} can be obtained if we can respectively derive the expressions of \bar{R}_1^{P} and \bar{R}_1^{S} .

We first calculate \bar{R}_1^{P} . Recall that in the PU-AS scheme, the maximum element of \mathbf{G} , i.e., g^{\max} , is first selected, and then the maximum element in the corresponding row of \mathbf{H} is subsequently selected. By using the i.i.d. property of the all the elements in \mathbf{H} , the PDF of $h_{n_p^*}^{\max}$ can be derived by using $f_{h^{\max}}(x)$. In this case, by given the PDF of g^{\max} in (28) and that of $h_{n_p^*}^{\max}$ in (22), an approximated expression of \bar{R}_1^{P} can be given in Proposition 3 as below.

Proposition 3. *With the QoS requirement of the primary user R_{th} and the distributions of g^{\max} and $h_{n_p^*}^{\max}$, the average rate of the secondary user UE₁ in PU-AS, i.e., \bar{R}_1^{P} , can be approximated in the high SNR regime as below:*

$$\begin{aligned} \bar{R}_1^{\text{P}} &\approx \sum_{i=1}^M \sum_{j=1}^{NK} \frac{(-1)^{i+j} \binom{M}{i} \binom{NK}{j}}{\ln 2} \\ &\quad \left(\frac{\varepsilon j \Omega_g}{i \Omega_h - \varepsilon j \Omega_g} \ln \frac{(\varepsilon + 1) j \Omega_g}{i \Omega_h + j \Omega_g} - \ln \frac{i \Omega_h}{\rho} - C \right). \end{aligned} \quad (45)$$

Proof: See Appendix D. ■

After obtaining \bar{R}_1^{P} , we thus turn to calculate \bar{R}_1^{S} for SU-AS. Recall that in SU-AS, the maximum element of \mathbf{H} (i.e., h^{\max}) is selected first, followed by the corresponding maximum element in the n_s^* row of \mathbf{G} (i.e., $g_{n_s^*}^{\max}$). Similarly, considering the i.i.d. property of the all the elements in \mathbf{G} , the PDF of $g_{n_s^*}^{\max}$ can be characterized by $f_{g^{\max}}(x)$. Given the PDF of h^{\max} in (26) and that of $g_{n_s^*}^{\max}$ in (24), the average rate of UE₁ in SU-AS, i.e., \bar{R}_1^{S} , is given by Proposition 4 as below.

Proposition 4. *With the QoS requirement of the primary UE and the distributions of h^{\max} and $g_{n_s^*}^{\max}$, respectively, the average rate of UE₁ in SU-AS, i.e., \bar{R}_1^{S} , can be approximated in the high SNR regime as below:*

$$\begin{aligned} \bar{R}_1^{\text{S}} &\approx \sum_{i=1}^{NM} \sum_{j=1}^K \frac{(-1)^{i+j} \binom{NM}{i} \binom{K}{j}}{\ln 2} \\ &\quad \left(\frac{\varepsilon j \Omega_g}{i \Omega_h - \varepsilon j \Omega_g} \ln \frac{(\varepsilon + 1) j \Omega_g}{i \Omega_h + j \Omega_g} - \ln \frac{i \Omega_h}{\rho} - C \right). \end{aligned} \quad (46)$$

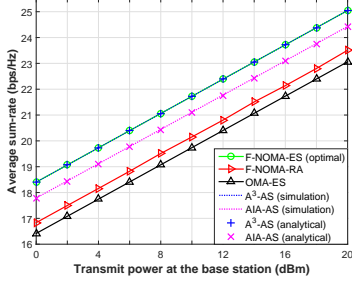


Fig. 1: Average sum-rate vs. transmit power in F-NOMA, $N = 2$, $d_1 = 80\text{m}$, $d_2 = 200\text{m}$, $a = 0.6$, $b = 0.4$.

Proof: Similar to Proposition 3, \bar{R}_1^S can be obtained by resolving the integral (11) over h^{\max} and $g_{n_s}^{\max}$. Comparing the distributions of h^{\max} and $g_{n_s}^{\max}$ in Proposition 4 to those of $h_{n_s}^{\max}$ and g^{\max} in Proposition 3, we can observe that the only difference between them lies in the corresponding upper limits of the summations. In this case, we can calculate \bar{R}_1^S by replacing the upper limits of i and j in (45) by NM and K , respectively. ■

Finally, by substituting (44)-(46) into (43), we can obtain an approximated closed-form expression for \bar{R}_1^{MCG} .

Remark 1. When the primary user UE_2 is much closer to the BS than the secondary user UE_1 , the event that $g^{\max} > h^{\max}$ occurs with a large probability. In this case, the MCG-AS scheme will reduce to the PU-AS scheme and thus $\bar{R}_1^{\text{MCG}} \approx \bar{R}_1^{\text{P}}$. On the other hand, when UE_2 is much further from the BS than UE_1 , it is more likely that $g^{\max} \leq h^{\max}$. In this case, the MCG-AS scheme degrades to SU-AS, and we have the approximation $\bar{R}_1^{\text{MCG}} \approx \bar{R}_1^{\text{S}}$.

V. NUMERICAL PERFORMANCE EVALUATIONS

In this section, the performance of the proposed joint AS algorithms for both F-NOMA and CR-NOMA systems is evaluated by using computer simulations and comparing to the benchmarks. In all simulations, we set $M = K = 2$, $\Omega_h = d_1^\alpha$, $\Omega_g = d_2^\alpha$, d_1 (d_2) is the distance between the BS and UE_1 (UE_2), the path-loss exponent $\alpha = 3$ and the variance of the noise is set as $\sigma^2 = -110\text{dBm}$.

A. Numerical Results for F-NOMA Systems

Fig. 1 illustrates how the transmit power P_s at the BS affects the system average sum-rate \bar{R}_{sum} . As can be observed from Fig. 1, when P_s increases, \bar{R}_{sum} increases for all the schemes. Moreover, the performance of the proposed A^3 -AS and AIA-AS schemes is much better than that of the random AS scheme in F-NOMA scenarios (F-NOMA-RA). Furthermore, the A^3 -AS scheme can achieve the same performance as that of the optimal ES scheme in F-NOMA scenarios (F-NOMA-ES) but with a much lower computational complexity. We should note that the analytical results match the simulation results for both A^3 -AS and AIA-AS, which validate our theoretical analysis in Sec. III. It is also worth pointing out that all the NOMA schemes outperform the ES scheme in OMA systems (OMA-ES) over the entire SNR region. For simplicity, we only show the analytical results in the following discussions.

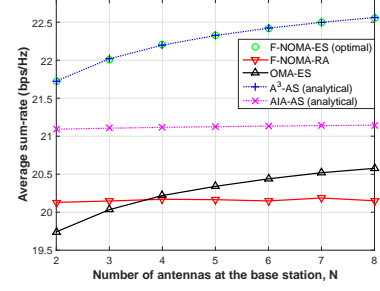


Fig. 2: Average sum-rate vs. N in F-NOMA, $d_1 = 80\text{m}$, $d_2 = 200\text{m}$, $a = 0.6$, $b = 0.4$, $P_s = 10\text{dBm}$.

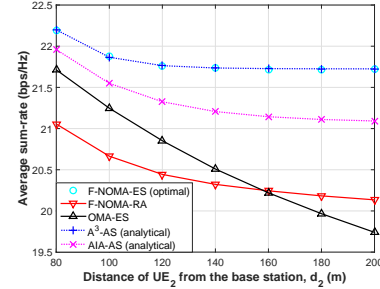


Fig. 3: Average sum-rate vs. d_2 in F-NOMA, $N = 2$, $d_1 = 80\text{m}$, $a = 0.6$, $b = 0.4$, $P_s = 10\text{dBm}$.

Fig. 2 illustrates how the number of antennas N at the BS influences the average sum-rate \bar{R}_{sum} . We can see from this figure that the sum-rates of F-NOMA-RA and AIA-AS keep constant when N increases. For the F-NOMA-RA scheme, this is because it does not properly utilize the multiple-antenna setting but selects one antenna at each node randomly. The reason why AIA-AS keeps constant is because it guarantees the performance of the *weak* user with the poor channel gain γ^w , but not the *strong* user with the better channel condition γ^s , which contributes the most to \bar{R}_{sum} . In contrast, the average sum-rate of A^3 -AS increases along with N , and A^3 -AS achieves the same performance as that of the optimal F-NOMA-ES scheme. Again, all the proposed NOMA schemes outperform the OMA-ES scheme in the entire region.

Fig. 3 depicts how the distances between the BS and users influence \bar{R}_{sum} for the schemes in F-NOMA systems. Take a constant d_1 and a variable d_2 for example. We can observe that when d_2 increases, \bar{R}_{sum} decreases for all the schemes in F-NOMA systems. We also note that both A^3 -AS and AIA-AS outperform the F-NOMA-RA and the OMA-ES schemes, and again A^3 -AS achieves almost the same performance as F-NOMA-ES. There is a crossing between the curves for F-NOMA-RA and OMA-ES. The reason for this is that in OMA-ES, when d_2 is much larger than d_1 , the energy and frequency resources allocated to UE_2 are wasted since they contribute very little to \bar{R}_{sum} .

Fig. 4 demonstrates how the power allocation coefficient b affects the \bar{R}_{sum} for various AS schemes in F-NOMA systems. Interestingly we can see that for all the F-NOMA schemes the average sum-rate keeps almost constant when b increases. The main reason is that $R_{\text{sum}} \approx \log(\gamma^s \rho)$ when $\rho \rightarrow \infty$; that is, the sum-rate is not affected by the value of b .

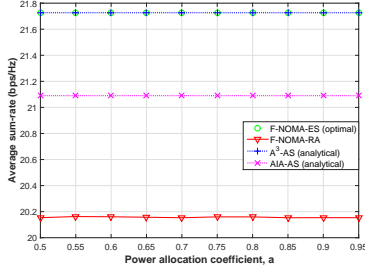


Fig. 4: Average sum-rate vs. a in F-NOMA, $N = 2, d_1 = 80\text{m}, d_2 = 200\text{m}, b = 1 - a, P_s = 10\text{dBm}$.

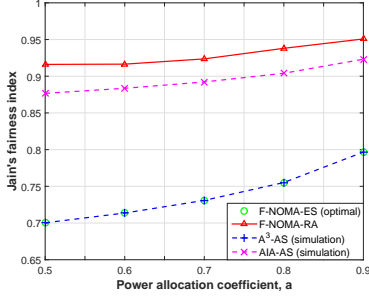


Fig. 5: Jain's fairness index vs. b in F-NOMA, $N = 4, d_1 = 80\text{m}, d_2 = 200\text{m}, b = 1 - a, P_s = 20\text{dBm}$.

Although the system sum-rate performance of A^3 -AS is shown to be slightly better than that of AIA-AS, regarding the fairness between UE_1 and UE_2 , we can observe in Fig. 5 that AIA-AS can provide better user fairness than A^3 -AS. In other words, in practice AIA-AS would be a better trade-off between the system throughput and user fairness.

B. Numerical Results for CR-NOMA Systems

In the considered two-user CR-NOMA down-link scenario, without loss of generality, we treat UE_2 as the PU and UE_1 as the SU. Fig. 6 illustrates how the locations of users affect the average rate of UE_1 . We now fix the location of the primary user UE_2 ($d_2 = 200\text{m}$) and place the secondary user UE_1 at various locations. As can be observed from Fig. 6, when d_1 increases, the average rate \bar{R}_1^c of UE_1 decreases for all the proposed AS schemes in CR-NOMA systems. Interestingly, there is a crossing for the curves of PU-AS and SU-AS around $d_1 = d_2 = 200\text{m}$. \bar{R}_1^c achieved by SU-AS is larger than that of PU-AS when $d_1 \leq 200\text{m}$ and the situation is reverse when $d_1 > 200\text{m}$. The reason is that when UE_1 is closer to the BS, the channel gain of UE_1 contributes more to \bar{R}_1^c , but when UE_2 is closer to the BS, the channel gain of UE_2 is more dominant to \bar{R}_1^c as more power is allocated to the secondary UE. Furthermore, MCG-AS, which takes advantage of PU-AS and SU-AS, can achieve almost the same performance as the optimal ES scheme in CR-NOMA scenarios (CR-NOMA-ES) for all the location settings but with much lower computational complexity, and all the proposed schemes outperform the random selection scheme in CR-NOMA scenarios (CR-NOMA-RA). It is worth pointing out that the analytical results match the simulation results for all the proposed CR-NOMA AS schemes, which validates our

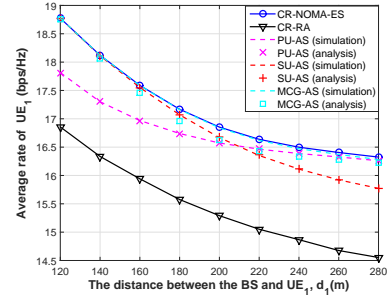


Fig. 6: Average rate of UE_1 vs. d_1 in CR-NOMA, $N = 4, d_2 = 200\text{m}, R_{\text{th}} = 5\text{bps/Hz}, P_s = 20\text{dBm}$.

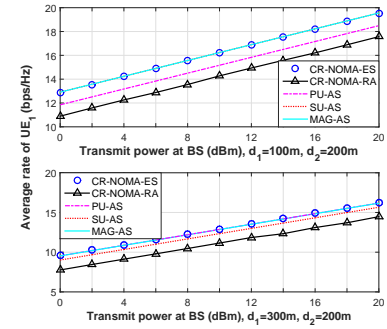


Fig. 7: Average rate of UE_1 vs. P_s in CR-NOMA, $N = 4, R_{\text{th}} = 5\text{bps/Hz}$.

theoretical analysis in Sec. IV. For brevity, we only show the analytical results in the following discussions.

Fig. 7 illustrates how the transmit power at the BS influences the achievable \bar{R}_1^c . We can see that when P_s increases, \bar{R}_1^c increases for all the schemes in CR-NOMA systems. Moreover, all the proposed AS schemes outperform CR-NOMA-RA. In particular, when UE_1 is closer to the BS, the performance of SU-AS is better than that of PU-AS. In contrast, when UE_2 is closer to the BS, the performances of SU-AS and PU-AS are inverted. Again MCG-AS achieves the near-optimal performance as CR-NOMA-ES in the entire region.

Fig. 8 illustrates how the number of antennas at the BS affects the achievable \bar{R}_1^c . When UE_1 is closer to the BS, the curve for SU-AS increases along with N . This is because in this case, the channel gain of UE_1 contributes more to \bar{R}_1^c and h_{nk} is maximized in SU-AS. In contrast, the curve for PU-AS keeps constant even when N increases. The reason for this is that PU-AS aims at maximizing the channel gain of UE_2 instead of UE_1 . That is, the channel gain of UE_1 is selected in a similar way to find out the maximum element from a random row of \mathbf{H} and h_{nk} is affected by M but not N . Interestingly, when UE_1 is farther from the BS than UE_2 , the aforementioned situation is inverted. Furthermore, all the proposed schemes outperform CR-NOMA-RA, and MCG-AS can achieve a near-optimal performance in the entire region.

Fig. 9 demonstrates how the QoS requirement R_{th} affects the achievable \bar{R}_1^c . We can see when R_{th} increases, the performances decrease for all the AS schemes in CR-NOMA. This is because when R_{th} increases, more power is allocated to UE_2 to meet the higher QoS requirement and

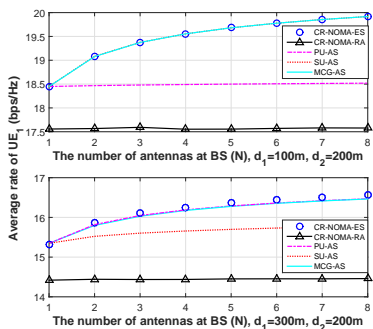


Fig. 8: Average rate of UE_1 vs. N in CR-NOMA, $P_s = 20\text{dBm}$, $R_{th} = 5\text{bps/Hz}$.

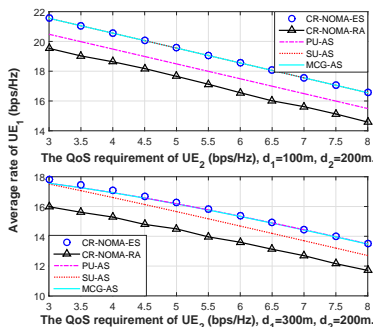


Fig. 9: Average rate of UE_1 vs. the QoS requirement of UE_2 in CR-NOMA, $N = 4$, $P_s = 20\text{dBm}$.

less power can be allocated to UE_1 . In this case, \bar{R}_1^c would decrease when R_{th} increases. Again, all the proposed AS schemes outperform CR-NOMA-RA, and MCG-AS achieves a near-optimal performance in the entire region. Moreover, the performance of PU-AS is better than that of SU-AS when UE_2 is closer to the BS, and it is opposite when UE_1 is closer to the BS.

As discussed above, MCG-AS can provide a near-optimal average rate performance for the SU in CR-NOMA networks by taking advantage of the instantaneous channel conditions of all the participants in systems. However, once the network-accessing priority and the near-far relationship of the users in CR-networks are determined, the PU-AS or SU-AS algorithms would be better choices. This is because the computational complexities of PU-AS and SU-AS are further lower than that of MCG-AS, and a near-optimal average rate performance for the secondary UE can be achieved by PU-AU when the primary user is much closer to the BS, and that is achieved by SU-AS when the secondary user is much closer to the BS.

VI. CONCLUSIONS

This paper studied the joint antenna selection (AS) problem for a classical MIMO-NOMA downlink communication scenario. Two computationally efficient AS algorithms, named A^3 -AS and AIA-AS, were proposed to maximize the system sum-rate of F-NOMA systems without and with the consideration of user fairness, respectively. Meanwhile, a low-complexity AS algorithm (i.e., MCG-AS) and its two simplified versions (i.e., PU-AS and SU-AS) were developed to maximize the rate of the SU in CR-NOMA systems. The

asymptotic closed-form expressions for the average sum-rates in F-NOMA systems and average rates of the secondary user in CR-NOMA systems were provided. Numerical simulations demonstrated that in F-NOMA systems, both A^3 -AS and AIA-AS yield significant performance gains over the random AS scheme and the OMA scheme with exhaustive search-based AS. Furthermore, A^3 -AS achieves the near-optimal sum-rate performance while AIA-AS provides better user fairness. In CR-NOMA scenarios, MCG-AS can achieve a near-optimal performance with much reduced complexity in the entire region. The complexities of the PU-AS and SU-AS is further lower than that of the MCG-AS scheme, while they only achieve a near-optimal performance when one user is much closer to the base station than the other.

APPENDIX A PROOF OF THE PROPOSITION 1

When $\rho \rightarrow \infty$, we can attain the asymptotic closed-form expression for the average sum-rate of the A^3 -AS algorithm as follows:

$$\begin{aligned} \bar{R}_{\text{sum}}^{A^3} &\approx \log \frac{1}{b} + \int_0^\infty \log(1 + b\rho_s x) f_{\gamma_{A^3}^s}(x) dx \stackrel{(c_2)}{=} \log \frac{1}{b} \\ &+ \sum_{i=1}^{NM} \sum_{j=1}^{NK} \frac{\mu_{i,NM} \mu_{j,NK}}{\ln 2} \left(e^{\frac{i\Omega_h + j\Omega_g}{b\rho}} \text{Ei} \left(-\frac{i\Omega_h + j\Omega_g}{b\rho} \right) \right. \\ &\quad \left. - e^{\frac{i\Omega_h}{b\rho}} \text{Ei} \left(-\frac{i\Omega_h}{b\rho} \right) - e^{\frac{j\Omega_g}{b\rho}} \text{Ei} \left(-\frac{j\Omega_g}{b\rho} \right) \right) \\ &\stackrel{(c_3)}{\approx} \log \frac{1}{b} + \sum_{i=1}^{NM} \sum_{j=1}^{NK} \frac{\mu_{i,NM} \mu_{j,NK}}{\ln 2} \left(\ln \left(\frac{i\Omega_h + j\Omega_g}{b\rho} \right) \right. \\ &\quad \left. - \ln \left(\frac{i\Omega_h}{b\rho} \right) - \ln \left(\frac{j\Omega_g}{b\rho} \right) - C \right) = \log \frac{1}{b} \\ &+ \sum_{i=1}^{NM} \sum_{j=1}^{NK} \frac{\mu_{i,NM} \mu_{j,NK}}{\ln 2} \left(\ln \left(\frac{i\Omega_h + j\Omega_g}{ij\Omega_h\Omega_g} \right) + \ln(b\rho) - C \right) \\ &\stackrel{(c_4)}{=} \frac{(\ln \rho - C)}{\ln 2} + \sum_{i=1}^{NM} \sum_{j=1}^{NK} \frac{\mu_{i,NM} \mu_{j,NK}}{\ln 2} \ln \left(\frac{i\Omega_h + j\Omega_g}{ij\Omega_h\Omega_g} \right) \quad (47) \end{aligned}$$

Specifically, the step (c_2) is obtained according to [33, Eq. (4.337.2)], the step (c_3) is obtained by applying the approximation $\text{Ei}(x) \stackrel{x \rightarrow 0}{\approx} C + \ln|x|$ [34] and the step (c_4) follows the property of the binomial coefficient $\sum_{i=0}^n (-1)^i \binom{n}{i} = 0$.

APPENDIX B PROOF OF THE LEMMA 1

In the first stage of AIA-AS, the maximum elements of each row from \mathbf{H} and \mathbf{G} , i.e., h_n^{\max} and g_n^{\max} , and their distributions are obtained according to (21)-(24). In the second stage of AIA-AS, the relatively smaller element $\gamma_n^w = \min(h_n^{\max}, g_n^{\max})$ in each row for $n \in \mathcal{N}$ is found out. Thus, the CDF of γ_n^w for $x \geq 0$ can be calculated as follows:

$$\begin{aligned} F_{\gamma_n^w}(x) &= \Pr \{ \min(h_n^{\max}, g_n^{\max}) < x \} \\ &= \Pr (h_n^{\max} < g_n^{\max} < x) + \Pr (g_n^{\max} < h_n^{\max} < x) \\ &= \int_0^x f_{g_n^{\max}}(y) \int_0^y f_{h_n^{\max}}(z) dz dy \\ &+ \int_0^x f_{h_n^{\max}}(y) \int_0^y f_{g_n^{\max}}(z) dz dy \\ &= 1 - \sum_{i=1}^M \sum_{j=1}^K \mu_{i,M} \mu_{j,K} e^{-(i\Omega_h + j\Omega_g)x}. \quad (48) \end{aligned}$$

In the third stage of AIA-AS, $\gamma_{\text{AIA}}^w = \max(\gamma_n^w)$ for $n \in \mathcal{N}$ is selected. In the case that γ_{AIA}^w lies in the n_{AIA}^* row, we first define $\hat{\gamma}^w = \max_{n \neq n_{\text{AIA}}^*} (\gamma_n^w)$ and obtain the CDF of $\hat{\gamma}^w$ as follows:

$$F_{\hat{\gamma}^w}(x) = [F_{\gamma_n^w}(x)]^{N-1} \stackrel{(c_6)}{=} \sum_{\ell} C_{\ell} t_{\ell} e^{-\xi_{\ell} x}, \quad (49)$$

where the step (c₆) is expanded according to the Multinomial theorem. Specifically, $\ell_0 + \dots + \ell_{MK} = N - 1$, the multinomial coefficient $C_{\ell} = \binom{N-1}{\ell_0, \dots, \ell_{MK}} = \frac{(N-1)!}{\ell_0! \dots \ell_{MK}!}$, $t_{\ell} = \prod_{1 \leq i \leq M} (-\mu_{i,M} \mu_{j,K})^{\ell_{ij}}$ and $\xi_{\ell} = \sum_{i=1}^M \sum_{j=1}^K (i\Omega_h + j\Omega_g) \ell_{ij}$.

Next we need to obtain the CDF and PDF of $\gamma_{\text{AIA}}^s = \max(h_{n_{\text{AIA}}^*}^{\max}, g_{n_{\text{AIA}}^*}^{\max})$ which lies in the same n_{AIA}^* row as γ_{AIA}^w . By applying some algebraic manipulations, we have

$$\begin{aligned} F_{\gamma_{\text{AIA}}^s}(x) &= \Pr \left\{ \max(h_{n_{\text{AIA}}^*}^{\max}, g_{n_{\text{AIA}}^*}^{\max}) < x, \gamma_{n_{\text{AIA}}^*}^w \geq \hat{\gamma}^w \right\} \\ &= N \left\{ \Pr(\hat{\gamma}^w < g_{n_{\text{AIA}}^*}^{\max} < h_{n_{\text{AIA}}^*}^{\max} < x) \right. \\ &\quad \left. + \Pr(\hat{\gamma}^w < h_{n_{\text{AIA}}^*}^{\max} < g_{n_{\text{AIA}}^*}^{\max} < x) \right\}, \quad (50) \end{aligned}$$

and

$$\begin{aligned} f_{\gamma_{\text{AIA}}^s}(x) &= N \left(f_{h_n^{\max}}(x) \int_0^x f_{g_n^{\max}}(y) \int_0^y f_{\hat{\gamma}^w}(z) dz dy \right. \\ &\quad \left. + f_{g_n^{\max}}(x) \int_0^x f_{h_n^{\max}}(y) \int_0^y f_{\hat{\gamma}^w}(z) dz dy \right), \end{aligned}$$

and by applying some algebraic operations, finally $f_{\gamma_{\text{AIA}}^s}(x)$ can be obtained as in (3A) APPENDIX C

PROOF OF THE PROPOSITION 2

Given the PDF of γ_{AIA}^s (i.e., $f_{\gamma_{\text{AIA}}^s}(x)$), we can approximate the average sum-rate of AIA-AS (i.e., $\bar{R}_{\text{sum}}^{\text{AIA}}$) according to (25) as below:

$$\begin{aligned} \bar{R}_{\text{sum}}^{\text{AIA}} &\approx \log \frac{1}{b} + \int_0^{\infty} \log(1 + b\rho x) f_{\gamma_{\text{AIA}}^s}(x) dx \quad (51) \\ &= \log \frac{1}{b} + \sum_{i=1}^M \sum_{j=1}^K \sum_{\ell} \frac{C_{\ell} t_{\ell}}{\ln 2} (T_1 + T_2 + T_3 + T_4), \end{aligned}$$

where T_1 is given by

$$\begin{aligned} T_1 &= - \int_0^{\infty} \frac{\xi_{\ell} \zeta_{ij} \ln(1 + b\rho x) e^{-j\Omega_g x}}{i\Omega_h \phi_i} dx \\ &\stackrel{(c_7)}{=} \frac{\xi_{\ell} \tilde{\zeta}_{ij}}{\phi_i} e^{\frac{j\Omega_g}{b\rho}} \text{Ei} \left(-\frac{j\Omega_g}{b\rho} \right) \stackrel{(c_8)}{\approx} \frac{\xi_{\ell} \tilde{\zeta}_{ij}}{\phi_i} \chi(j\Omega_g), \quad (52) \end{aligned}$$

in which $\tilde{\zeta}_{ij} = N\mu_{i,M}\mu_{j,K}$, $\phi_i = i\Omega_h + \xi_{\ell}$, $\chi(x) = C + \ln|\frac{x}{b\rho}|$, Ei(x) is the Exponential integral function and $C \approx 0.577$ is the Euler's constant. Specifically, the step (c₇) is obtained with the help of [33, Eq. (4.337.2)], and the step (c₈) is obtained by using the approximation of $e^x \approx 1$ and Ei(x) $\approx C + \ln x$ when $x \rightarrow 0$ [34]. Similarly,

$$\begin{aligned} T_2 &= - \int_0^{\infty} \frac{\xi_{\ell} \zeta_{ij} \ln(1 + b\rho x) e^{-i\Omega_h x}}{j\Omega_g \phi_j} dx = \frac{\xi_{\ell} \tilde{\zeta}_{ij}}{\phi_j} \chi(i\Omega_h), \\ T_3 &= - \int_0^{\infty} \frac{\zeta_{ij} \phi_{ij,2} \ln(1 + b\rho x) e^{-\phi_{ij,1} x}}{\phi_i \phi_j} dx = \frac{\zeta_{ij} \phi_{ij,2} \chi(\phi_{ij,1})}{\phi_i \phi_j \phi_{ij,1}}, \\ T_4 &= \int_0^{\infty} \frac{\zeta_{ij} (i\Omega_h + j\Omega_g) \ln(1 + b\rho x) e^{-(i\Omega_h + j\Omega_g) x}}{ij\Omega_h \Omega_g} dx \\ &= -\tilde{\zeta}_{ij} \chi(i\Omega_h + j\Omega_g), \end{aligned}$$

in which, $\phi_j = j\Omega_g + \xi_{\ell}$, $\phi_{ij,1} = i\Omega_h + j\Omega_g + \xi_{\ell}$, and $\phi_{ij,2} = i\Omega_h + j\Omega_g + 2\xi_{\ell}$.

APPENDIX D

PROOF OF THE PROPOSITION 3

Recall that the achievable rate of the secondary user in (11) consists of two terms. Here we can calculate the asymptotic average rate of UE₁ in PU-AS, which is denoted by $\bar{R}_1^{\text{P}} = \mathbb{E}[R_1^{\text{P}}]$, in two parts.

The first part of (11), i.e., $\bar{R}_{1,1}^{\text{P}}$, can be obtained by calculating the following integral for $\delta_{n^*, m^*, k^*} = 1$:

$$\begin{aligned} \bar{R}_{1,1}^{\text{P}} &= \int_0^{\infty} \int_0^x \log \left(\frac{\rho x}{\varepsilon + 1} \right) f_{g^{\max}}(y) f_{h_n^{\max}}(x) dy dx \\ &= \sum_{i=1}^M \sum_{j=1}^{NK} \frac{i\Omega_h \mu_{i,M} \mu_{j,NK}}{\ln 2} \left\{ \int_0^{\infty} \ln \left(\frac{\rho x}{\varepsilon + 1} \right) e^{-i\Omega_h x} dx \right. \\ &\quad \left. - \int_0^{\infty} \ln \left(\frac{\rho x}{\varepsilon + 1} \right) e^{-(i\Omega_h + j\Omega_g) x} dx \right\} \\ &\stackrel{y=\rho x/(\varepsilon+1)}{=} \sum_{i=1}^M \sum_{j=1}^{NK} \frac{i(\varepsilon + 1)\Omega_h \mu_{i,M} \mu_{j,NK}}{\rho \ln 2} \left\{ \int_0^{\infty} \ln y e^{-\frac{(\varepsilon+1)i\Omega_h y}{\rho}} dy \right. \\ &\quad \left. - \int_0^{\infty} \ln y e^{-\frac{(\varepsilon+1)(i\Omega_h + j\Omega_g) y}{\rho}} dy \right\} \\ &\stackrel{(c_9)}{=} \sum_{i=1}^M \sum_{j=1}^{NK} \frac{\mu_{i,M} \mu_{j,NK}}{\ln 2} \left\{ -C - \ln \left(\frac{i(\varepsilon + 1)\Omega_h}{\rho} \right) \right. \\ &\quad \left. + \frac{i\Omega_h C}{i\Omega_h + j\Omega_g} + \frac{i\Omega_h \ln \left(\frac{(\varepsilon+1)(i\Omega_h + j\Omega_g)}{\rho} \right)}{i\Omega_h + j\Omega_g} \right\} \\ &= \sum_{i=1}^M \sum_{j=1}^{NK} \frac{\mu_{i,M} \mu_{j,NK}}{\ln 2} \left\{ -\ln(i\Omega_h) \right. \\ &\quad \left. + \frac{j\Omega_g \left(\ln \left(\frac{\rho}{\varepsilon+1} \right) - C \right) + i\Omega_h \ln(i\Omega_h + j\Omega_g)}{i\Omega_h + j\Omega_g} \right\}. \quad (53) \end{aligned}$$

Specifically, the step (c₉) is obtained with the help of [33, Eq. (4.331.1)].

The second part of (11), i.e., $\bar{R}_{1,2}^{\text{P}}$, can be obtained by calculating the following integral for $\delta_{n^*, m^*, k^*} = 0$:

$$\begin{aligned} \bar{R}_{1,2}^{\text{P}} &= \int_0^{\infty} \int_x^{\infty} \log \left(\frac{\rho xy}{\varepsilon x + y} \right) f_{g^{\max}}(y) dy f_{h_n^{\max}}(x) dx \\ &= \underbrace{\int_0^{\infty} \int_x^{\infty} \log(\rho x) f_{g^{\max}}(y) dy f_{h_n^{\max}}(x) dx}_{T_5} \\ &\quad + \underbrace{\int_0^{\infty} \int_x^{\infty} \log(y) f_{g^{\max}}(y) dy f_{h_n^{\max}}(x) dx}_{T_6} \\ &\quad - \underbrace{\int_0^{\infty} \int_x^{\infty} \log(\varepsilon x + y) f_{g^{\max}}(y) dy f_{h_n^{\max}}(x) dx}_{T_7}, \quad (54) \end{aligned}$$

in which,

$$\begin{aligned} T_5 &= \sum_{i=1}^M \sum_{j=1}^{NK} \frac{ij\Omega_h \Omega_g \mu_{i,M} \mu_{j,NK}}{\ln 2} \int_0^{\infty} \int_x^{\infty} \ln(\rho x) e^{-j\Omega_g y} dy e^{-i\Omega_h x} dx \\ &= \sum_{i=1}^M \sum_{j=1}^{NK} \frac{i\Omega_h \mu_{i,M} \mu_{j,NK}}{\ln 2} \int_0^{\infty} \ln(\rho x) e^{-(i\Omega_h + j\Omega_g) x} dx \\ &\stackrel{(c_{10})}{=} \sum_{i=1}^M \sum_{j=1}^{NK} \frac{\mu_{i,M} \mu_{j,NK}}{\ln 2} \frac{(-i\Omega_h (C + \ln(i\Omega_h + j\Omega_g)) - \ln \rho)}{\ln 2 (i\Omega_h + j\Omega_g)}, \quad (55) \end{aligned}$$

where the step (c_{10}) is obtained with the help of the substitution $t = \rho x$ and that of [33, Eq. (4.331.1)]. Similarly,

$$\begin{aligned}
T_6 &= \sum_{i=1}^M \sum_{j=1}^{NK} \frac{ij\Omega_h\Omega_g\mu_{i,M}\mu_{j,NK}}{\ln 2} \int_0^\infty \int_x^\infty \ln ye^{-j\Omega_g y} dy e^{-i\Omega_h x} dx \\
&\stackrel{(c_{11})}{=} \sum_{i=1}^M \sum_{j=1}^{NK} \frac{i\Omega_h\mu_{i,M}\mu_{j,NK}}{\ln 2} \int_0^\infty \left(\ln xe^{-j\Omega_g x} \right. \\
&\quad \left. - \text{Ei}(-j\Omega_g x) \right) e^{-i\Omega_h x} dx \\
&\stackrel{(c_{12})}{=} \sum_{i=1}^M \sum_{j=1}^{NK} \frac{\mu_{i,M}\mu_{j,NK}}{\ln 2} \left(\ln(i\Omega_h + j\Omega_g) \right. \\
&\quad \left. - \ln(j\Omega_g) - \frac{i\Omega_h(C + \ln(i\Omega_h + j\Omega_g))}{i\Omega_h + j\Omega_g} \right), \tag{56}
\end{aligned}$$

where the step (c_{11}) is calculated with the substitution $t = y/x$ and [33, Eq. (4.331.2)], and the step (c_{12}) is with [35, Eq. (2.5.3.1)]. For the T_7 , we have

$$\begin{aligned}
T_7 &= \sum_{i=1}^M \sum_{j=1}^{NK} \frac{ij\Omega_h\Omega_g\mu_{i,M}\mu_{j,NK}}{\ln 2} \int_0^\infty \int_x^\infty \ln(\varepsilon x + y) \\
&\quad e^{-j\Omega_g y} dy e^{-i\Omega_h x} dx \\
&\stackrel{t=y-x}{=} \sum_{i=1}^M \sum_{j=1}^{NK} \frac{ij\Omega_h\Omega_g\mu_{i,M}\mu_{j,NK}}{\ln 2} \int_0^\infty \int_0^\infty \ln((\varepsilon + 1)x + t) \\
&\quad e^{-j\Omega_g t} dt e^{-(i\Omega_h + j\Omega_g)x} dx \\
&\stackrel{(c_{13})}{=} \sum_{i=1}^M \sum_{j=1}^{NK} \frac{i\Omega_h\mu_{i,M}\mu_{j,NK}}{\ln 2} \int_0^\infty \left(\ln(\varepsilon + 1) + \ln x \right. \\
&\quad \left. - \text{Ei}[-j\Omega_g(\varepsilon + 1)x] e^{j\Omega_g(\varepsilon + 1)x} \right) e^{-(i\Omega_h + j\Omega_g)x} dx \\
&\stackrel{(c_{14})}{=} \sum_{i=1}^M \sum_{j=1}^{NK} \frac{\mu_{i,M}\mu_{j,NK}}{\ln 2} \left(\frac{i\Omega_h(\ln(\varepsilon + 1) - C - \ln(i\Omega_h + j\Omega_g))}{i\Omega_h + j\Omega_g} \right) \\
&\quad + \frac{i\Omega_h(\ln(i\Omega_h + j\Omega_g) - \ln((\varepsilon + 1)j\Omega_g))}{i\Omega_h - \varepsilon j\Omega_g} \tag{57}
\end{aligned}$$

where the step (c_{13}) is with [33, Eq. (4.337.1)] and the step (c_{14}) is with [33, Eq. (4.331.1)] and [35, Eq. (2.5.3.1)].

In this case, we can obtain $\bar{R}_{1,2}^P$ by summing up (55)-(57), and obtain \bar{R}_1^P by summing up (53) and (54). After some manipulations, \bar{R}_1^P can be obtained as in (45).

REFERENCES

- [1] Y. Yu, *et al.*, "Antenna selection for MIMO-NOMA networks", in *2017 IEEE Int. Conf. Commun. (ICC)*, May 2017.
- [2] Y. Saito, *et al.*, "Non-orthogonal multiple access (NOMA) for cellular future radio access", in *Proc. IEEE Veh. Technol. Conf. (VTC Spring)*, Jun. 2013.
- [3] L. Dai, *et al.*, "Non-orthogonal multiple access for 5G: solutions, challenges, opportunities, and future research trends", *IEEE Commun. Mag.*, vol. 53, pp. 74-81, Sep. 2015.
- [4] Z. Wei, *et al.*, "A survey of downlink non-orthogonal multiple access for 5G wireless communication networks", arXiv: 1609. 01856, 2016.
- [5] Z. Ding, *et al.*, "On the performance of non-orthogonal multiple access in 5G systems with randomly deployed users", *IEEE Signal Process. Lett.*, vol. 21, pp. 1501-1505, Dec. 2014.
- [6] J. Choi, "Non-orthogonal multiple access in downlink coordinated two-point systems", *IEEE Commun. Lett.*, vol. 18, pp. 313-316, Jan. 2014.
- [7] M. Al-lmari, *et al.*, "Uplink non-orthogonal multiple access for 5G wireless networks", in *11th Int. Symposium on Wireless Commun. Systems (ISWCS)*, pp. 781-785, Aug. 2014.
- [8] J. Kim, and I. Lee, "Non-orthogonal multiple access in coordinated direct and relay transmission", *IEEE Commun. Lett.*, vol. 19, pp. 2037-2040, Aug. 2015.
- [9] Y. Sun, *et al.*, "Optimal joint power and sub-carrier allocation for full-duplex multi-carrier non-orthogonal multiple access systems", arXiv: 1607. 02668, 2016.
- [10] Y. Liu, *et al.*, "Non-orthogonal multiple access in large-scale underlay cognitive radio networks", *IEEE Trans. Veh. Technol.*, Mar. 2016
- [11] Z. Dong, *et al.*, "On non-orthogonal multiple access with finite-alphabet inputs in Z-channels", *IEEE J. Sel. Commun.*, 2017.
- [12] W. Bao, *et al.*, "Joint rate control and power allocation for non-orthogonal multiple access systems." arXiv:1705.08572, 2017.
- [13] Z. Ding, F. Adachi, H. V. Poor, "The application of MIMO to non-orthogonal multiple access", *IEEE Trans. Wireless Commun.*, vol. 15, no. 1, Jan. 2016.
- [14] Q. Sun, *et al.*, "On the ergodic capacity of MIMO NOMA systems", *IEEE Wireless Commun. Lett.*, vol. 4, no. 4, Aug. 2015.
- [15] Z. Ding and H. V. Poor, "Design of massive-MIMO-NOMA with limited feedback", arXiv: 1511. 05583, 2015.
- [16] B. Kim, *et al.*, "Non-orthogonal multiple access in a downlink multi-user beam-forming system", in *IEEE Military Commun. Conf. (MILCOM)*, pp. 1278-1283, Nov. 2013.
- [17] Y. Liu, *et al.*, "Fairness of user clustering in MIMO non-Orthogonal multiple access systems", *IEEE Commun. Lett.*, vol. 20, pp. 1465-1468, Apr. 2016.
- [18] A. F. Molish and M. Z. Win, "MIMO systems with antenna selection", *IEEE Micro. Mag.*, vol. 5, pp. 46-56, Mar. 2004.
- [19] R. Zhang and Y. C. Liang, "Exploiting multi-antennas for opportunistic spectrum sharing in cognitive radio networks", *IEEE J. Sel. Topics Signal Process.*, vol. 2, pp. 88-102, Feb. 2008.
- [20] S. Sanayei, and A. Nosratinia, "Antenna selection in MIMO systems", *IEEE Commun. Mag.*, vol. 42, pp. 68-73, Oct. 2004.
- [21] A. P. Shrestha, *et al.*, "Performance of transmit antenna selection in non-orthogonal multiple access for 5G systems", in *8th Int. Conf. on Ubiquitous and Future Netw. (ICUFN)*, Jul. 2016.
- [22] X. Liu and X. Wang, "Efficient antenna selection and user scheduling in 5G massive MIMO-NOMA system", in *Proc. IEEE Veh. Technol. Conf. (VTC Spring)*, May 2016.
- [23] Z. Ding, P. Fan and H. V. Poor, "Impact of user pairing on 5G nonorthogonal multiple-access downlink transmissions", *IEEE Trans. Veh. Technol.*, vol. 65, no. 8, pp. 6010-6023, Aug. 2016.
- [24] Z. Ding, R. Schober, and H. V. Poor, "A general MIMO framework for NOMA downlink and uplink transmission based on signal alignment", *IEEE Trans. Wireless Commun.*, vol. 15, no. 6, pp. 4438-4454, Mar. 2016.
- [25] Z. Ding, L. Dai, and H. V. Poor, "MIMO-NOMA design for small packet transmission in the Internet of Things", *IEEE Access*, vol. 4, pp. 1393-1405, 2016.
- [26] K. Tourki, *et al.*, "Exact performance analysis of MIMO cognitive radio systems using transmit antenna selection", *IEEE J. Sel. Commun.*, vol. 32, no. 3, pp. 425-438, 2014
- [27] K. Song, *et al.*, "Performance analysis of antenna Selection in two-way relay networks", *IEEE Trans. Signal Process.*, vol. 63, no. 10, pp. 2520-2532, 2015.
- [28] R. K. Jain, *et al.*, "A quantitative measure of fairness and discrimination for resource allocation in shared computer systems", *DEC Technical Report 301*, Sept. 1984.
- [29] Y. Liu, *et al.*, "Non-orthogonal multiple access in large-scale heterogeneous networks", arXiv:1705.03325, 2017.
- [30] S. Timotheou, and I. Krikidis, "Fairness for non-orthogonal multiple access in 5G systems", *IEEE Signal Processing Letters*, vol. 22, no. 10, pp. 1647-1651, 2015.
- [31] J. Zhao, *et al.*, "Spectrum allocation and power control for non-orthogonal multiple access in HetNets", *IEEE Trans. on Wireless Commun.*, 2017.
- [32] S. Shinjo, *et al.*, "Integrating the front end: a highly integrated RF front end for high-SHF wide-band massive MIMO in 5G", *IEEE Microwave Magazine*, vol. 18, no. 5, 2017.
- [33] I. S. Gradshteyn and I. M. Ryzhik, *Table of integrals, series, and products*, 6th ed., Academic press, 2000.
- [34] W. J. Cody, and H. C. Thacher, "Chebyshev approximations for the exponential integral $Ei(x)$ ", *Mathematics of Computation*, 1969.
- [35] A. P. Prudnikov, Y. A. Brychkov, and O. I. Marichev, *Integrals and series (volume 2: special functions)*, Gordon and breach science publishers, 1983.